RESEARCH ARTICLE

ENERGY HARVESTING

Harvesting electrical energy from carbon nanotube yarn twist

Shi Hyeong Kim,[1,2]* Carter S. Haines,[2]* Na Li,[2]* Keon Jung Kim,[1] Tae Jin Mun,[1] Changsoon Choi,[1] Jiangtao Di,[2] Young Jun Oh,[3] Juan Pablo Oviedo,[3] Julia Bykova,[4] Shaoli Fang,[2] Nan Jiang,[5] Zunfeng Liu,[5,6] Run Wang,[5,6] Prashant Kumar,[7] Rui Qiao,[7] Shashank Priya,[7] Kyeongjae Cho,[3] Moon Kim,[3] Matthew Steven Lucas,[8] Lawrence F. Drummy,[8] Benji Maruyama,[8] Dong Youn Lee,[1] Xavier Lepró,[2] Enlai Gao,[2] Dawood Albarq,[2] Raquel Ovalle-Robles,[4] Seon Jeong Kim,[1]† Ray H. Baughman[2]†

Mechanical energy harvesters are needed for diverse applications, including self-powered wireless sensors, structural and human health monitoring systems, and the extraction of energy from ocean waves. We report carbon nanotube yarn harvesters that electrochemically convert tensile or torsional mechanical energy into electrical energy without requiring an external bias voltage. Stretching coiled yarns generated 250 watts per kilogram of peak electrical power when cycled up to 30 hertz, as well as up to 41.2 joules per kilogram of electrical energy per mechanical cycle, when normalized to harvester yarn weight. These energy harvesters were used in the ocean to harvest wave energy, combined with thermally driven artificial muscles to convert temperature fluctuations to electrical energy, sewn into textiles for use as self-powered respiration sensors, and used to power a light-emitting diode and to charge a storage capacitor.

The importance of harvesting mechanical energy as electrical energy motivates the search for new technologies. Electromagnetic electric energy generators suffer from low power densities and high cost per watt when scaled to the millimeter and smaller dimensions needed for emerging applications (*1*). Piezoelectric and ferroelectric harvesters work well for high-frequency, low-strain deformations (*2*), especially when individual nanofibers are driven at ultrahigh resonant frequencies (*3*), but they lack the elasticity needed for harvesting large strains. Triboelectric harvesters (*4*, *5*) perform well and are promising for future applications. Harvesters that use the coupling between flowing fluids and electronic charge are appealing (*6*–*8*) but need improvements in output power. Diverse electrochemical harvesters are known—including conducting polymer harvesters (*9*), lithium battery–based bending harvesters (*10*), and ionic polymer–metal composite harvesters (*11*)—but have not yet provided competitive performance. The capacitance change caused by mechanically altering the area of liquid contact with two charged or self-charged capacitor electrodes has been used for dielectric (*12*) and electrochemical (*13*) energy harvesting, but these technologies are still in early development.

Rubber-based dielectric capacitors are attractive for converting large-stroke mechanical energy into electricity. A thin elastomeric sheet is sandwiched between two deformable electrodes (*14*, *15*). An applied voltage (V), typically ~1000 V, is used to inject charge (Q) into this elastomeric capacitor. When stretched, the rubber dielectric decreases thickness, increasing capacitance (C) and thereby producing a voltage change according to $Q = CV$, which enables electrical energy generation.

To avoid these high voltages and associated circuits, we previously tried to manufacture a twisted carbon nanotube (CNT) yarn mechanical energy harvester that electrochemically generated electrical energy when stretched. However, even when volt-scale positive or negative bias voltages were applied, tensile stresses of up to 45 MPa resulted in such small short circuit currents that the only possible application was as an externally powered strain sensor (*16*).

Fabrication and performance of CNT yarn harvesters

We demonstrate CNT yarns that can be stretched to generate a peak electrical power of 250 W per kilogram of yarn, without needing an external bias voltage. This advance resulted in part from our transitioning from CNT yarns that are twisted but not coiled to yarns that are so highly twisted that they completely coil, which we hereafter refer to as twisted and coiled yarns, respectively.

Harvesters were produced by spinning sheets of forest-drawn carbon multiwalled nanotubes (MWNTs) into high-strength yarns (*17*, *18*). Due to large MWNT diameters, MWNT bundling, and the absence of pseudo-capacitive redox groups, these yarns have a capacitance of <15 F/g (*19*). By inserting extreme twist into a CNT yarn that supports a weight, coils initiate and propagate, producing a highly elastic, uniformly coiled structure. Figure 1A illustrates the spinning methods and resulting yarn topologies before the onset of coiling. Unless otherwise noted, the harvester yarns had a diameter of 50 to 70 μm when twisted to just before coiling and were made by the cone–spinning process depicted in Fig. 1A. F1

Figure 1B illustrates the electrochemical cell used for the initial characterization of harvester yarns; this cell comprises a coiled MWNT yarn working electrode, a high-surface-area counter electrode, and a reference electrode, all of which are immersed in aqueous electrolyte. Figure 1C shows the time dependence of open-circuit voltage (OCV) and short-circuit current (SCC) generated by a coiled cone-spun harvester during 1-Hz sinusoidal stretch to 30% strain in 0.1 M HCl electrolyte. This sinusoidal stretch does not produce sinusoidal variation in OCV or SCC if the applied tension is so low that the yarn is not in an extended configuration, because the input mechanical energy per change in strain (and corresponding output voltage and electrical energy change) is reduced by a low effective yarn stiffness. Because the voltage peaks most sharply when the yarn is fully stretched, peak power can exceed average power by an observed factor as high as 3.34, as compared with the factor of 2 expected for a purely sinusoidal voltage profile.

When stretched to 30% strain, the harvester's capacitance decreased 30.7%, and its OCV increased by 140 mV (Fig. 1D). Unless otherwise noted herein, the electrolyte is 0.1 M HCl, the reference electrode is Ag/AgCl, and the applied strain is sinusoidal. Applied tensile stresses are normalized to the cross-sectional area of the twisted, noncoiled yarn.

Harvester performance has been improved by using the hysteretic nature of twist insertion and removal (fig. S23): Untwisting a coiled yarn by a small amount does not result in coil loss but instead increases coil diameter and reduces twist-induced densification. As shown in Fig. 1, E and F, and fig. S6, untwisting by 500 turns/m (8.5% of the twist inserted to fully coil) increased the reversible tensile strain range from 30 to 50% and increased the tensile strain–induced capacitance change from 30 to 36%. The capacitance at 0% strain increased from 3.97 to 6.50 F/g, due to the reduced compressive forces and decreased yarn density resulting from twist removal. Most importantly, this twist removal increased peak power at 12 Hz by a factor of 1.4 (peak power increased to 179 W/kg, which is 30.97 μW for this 0.173-mg harvester) (fig. S11) and increased maximum output energy per cycle at 0.25 Hz

[1]Center for Self-Powered Actuation, Department of Biomedical Engineering, Hanyang University, Seoul 04763, South Korea. [2]Alan G. MacDiarmid NanoTech Institute, University of Texas at Dallas, Richardson, TX 75080, USA. [3]Department of Materials Science and Engineering, University of Texas at Dallas, Richardson, TX 75080, USA. [4]Lintec of America, Nano-Science & Technology Center, Richardson, TX 75081, USA. [5]Jiangnan Graphene Research Institute, Changzhou 213149, China. [6]State Key Laboratory of Medicinal Chemical Biology, College of Pharmacy, Nankai University, Tianjin, 300071, China. [7]Department of Mechanical Engineering, Virginia Polytechnic Institute and State University, Blacksburg, VA 24061, USA. [8]Air Force Research Laboratory, Materials and Manufacturing Directorate, Wright-Patterson Air Force Base, Dayton, OH 45433, USA.
*These authors contributed equally to this work. †Corresponding author. Email: sjk@hanyang.ac.kr (S.J.K.); ray.baughman@utdallas.edu (R.H.B.)

by a factor of 2.9 (per-cycle energy increased to 41.2 J/kg, which is 7.13 μJ) (Fig. 1E). The existence of a long plateau in frequencies that maximize power (from 12 Hz to >25 Hz in Fig. 1E) provides a major advantage compared with resonant harvesters, whose power output rapidly degrades as mechanical deformation frequencies deviate from resonance (*20*).

The above performance was obtained for CNT yarn electrodes produced by a twist-insertion process called cone spinning; this process optimizes harvester performance. Unlike for conventional "dual-Archimedean" yarn fabrication, in which twisting a rectangular stack of CNT sheets between fixed supports causes a gradient of tension along the sheet width (*21*), cone spinning (Fig. 1A and fig. S1) maintains quasi-uniform tension across the CNT array. This stress nonuniformity was avoided by rolling a CNT sheet stack about the CNT alignment direction to make a cylinder (*22*) and then twisting this cylinder around its central axis to produce two cones, which densify to a yarn. These quasi-uniformly twisted yarns produced roughly four times the peak power and average power generated by dual-Archimedean yarns (Fig. 2A, table S1, and fig. S25). Similarly, methods such as tow spinning, funnel spinning, and Fermat spinning (Fig. 1A) (*22*) also reduced nonuniform tension during twisting and provided comparably high-performance yarns.

For a given inserted twist, the mechanical load applied during twisting determines the coil spring index (*22*), which affects harvester performance. The peak power and change in capacitance for a given percent strain are optimized for a spring index of ~0.43 (measured after coiling, with the coiling load still applied), which yielded a peak power of 41.3 W/kg for 30% strain at 1 Hz (fig. S2). However, as the spring index increases, the maximum reversible coil deformation increases (and the coil stiffness decreases), enabling energy harvesting over a larger strain range. This tunability allows the harvester to be customized for the stroke range needed for a particular application. Unless otherwise indicated, a spring index of ~0.43 was used for all experiments.

For potential use in harvesting the energy in ocean waves, CNT yarn harvesters were tested in 0.6 M NaCl, a concentration similar to that found in seawater. For 30% stretch and deformation frequencies of 0.25 to 12 Hz, a plateau in peak power (at ~94 W/kg) was observed above 6 Hz (fig. S10). As needed for ocean-wave harvesting, harvester performance in 0.6 M NaCl (and in 0.1 M HCl) varies little with temperature (figs. S13 and S24). Also, the peak power and the load resistance that optimizes peak power depend little on NaCl concentrations between 0.6 and 5 M, and the peak power decreases by less than 20% for concentrations down to 0.1 M (fig. S9), which means that these harvesters can be used for ocean environments of varying salinity. Figure 2B shows that the peak power and average power at 0°C (46.3 and 15.3 W/kg) were maintained for more than 30,000 cycles at 1 Hz to 30% strain in 0.6 M NaCl.

Important for many applications, gravimetric energy output per cycle is scale-invariant, as shown for coiled harvester yarns in fig. S7. The amount of inserted twist (*T*, in turns per meter) was scaled inversely with yarn diameter *D* to keep *TD* constant. This structural scaling automatically occurred because yarns were twisted under the same stress until fully coiled, and *TD* was scale-invariant for this degree of inserted twist. Likewise, the obtained spring index (presently 0.43) was scale-invariant. The per-cycle gravimetric energy, peak-to-peak OCV, and frequency dependence of gravimetric peak power were constant for yarn diameters between 40 and 110 μm (fig. S7). Also, a similar peak power density was obtained at 1 Hz for a coiled yarn and a four-ply yarn made from this coiled yarn (fig. S18).

We call our devices "twistron" harvesters—"twist" denotes the harvester mechanism, and "tron" is the Greek suffix for device. The twist mechanism for energy harvesting by stretching a coiled yarn was first suggested by our observation that twisting a noncoiled yarn generated electrical

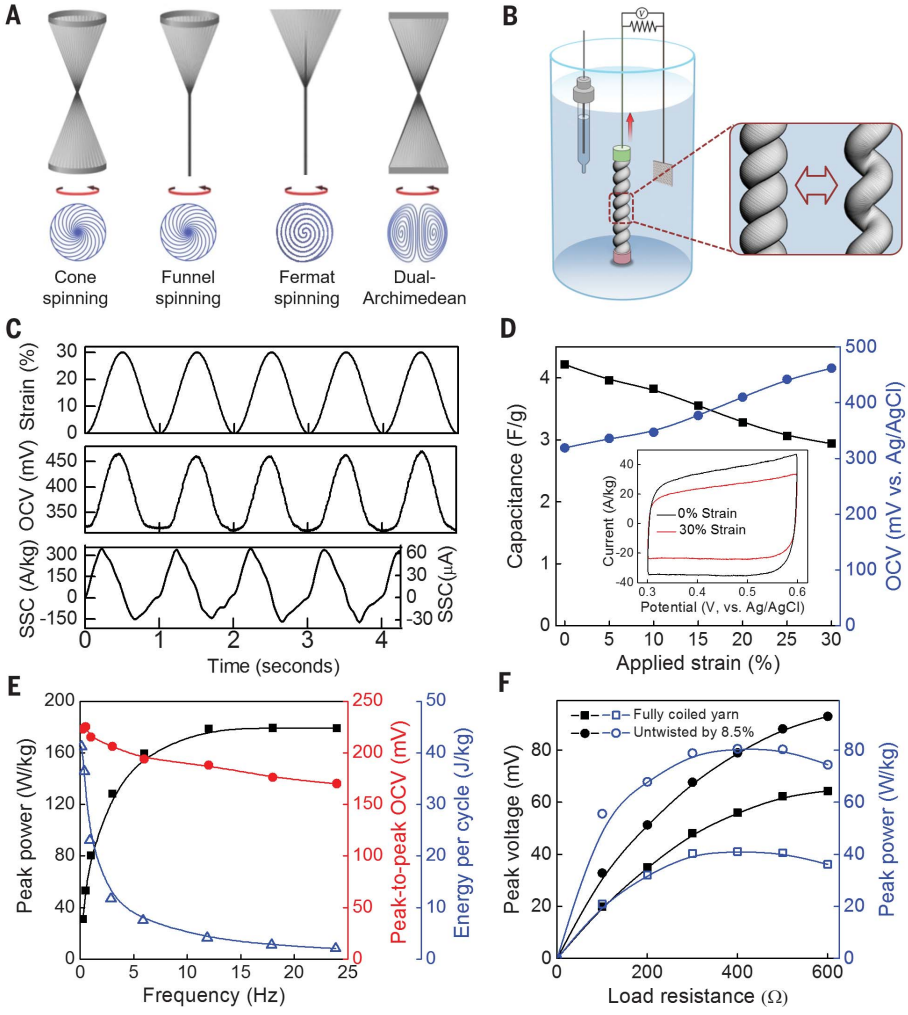

Fig. 1. Twistron harvester configuration, structure, and performance for tensile energy harvesting in 0.1 M HCl. (**A**) Illustrations of cone, funnel, Fermat, and dual-Archimedean spinning (top) and resulting yarn cross sections (bottom). (**B**) Illustration of a torsionally tethered coiled harvester electrode and counter and reference electrodes in an electrochemical bath, showing the coiled yarn before and after stretch. (**C**) Sinusoidal applied tensile strain and resulting change in open-circuit voltage (OCV) and short-circuit current (SCC) before (right) and after (left) normalization for a cone-spun coiled harvester. (**D**) Capacitance and OCV versus applied strain for the harvester of (C). (Inset) Cyclic voltammetry curves for 0 and 30% strain. (**E**) Frequency dependence of peak power (solid black squares), peak-to-peak OCV (solid red circles), and energy per cycle (open blue triangles) for 50% stretch of an 8.5%-untwisted coiled harvester. The output electrical power from this 0.173-mg twistron harvester electrode is 31.0 μW above 10 Hz. (**F**) Generated peak power (solid black symbols) and peak voltage (open blue symbols) versus load resistance for a coiled yarn (squares) and a partially untwisted coiled yarn (circles) when stretched at 1 Hz to the maximum reversible elongation.

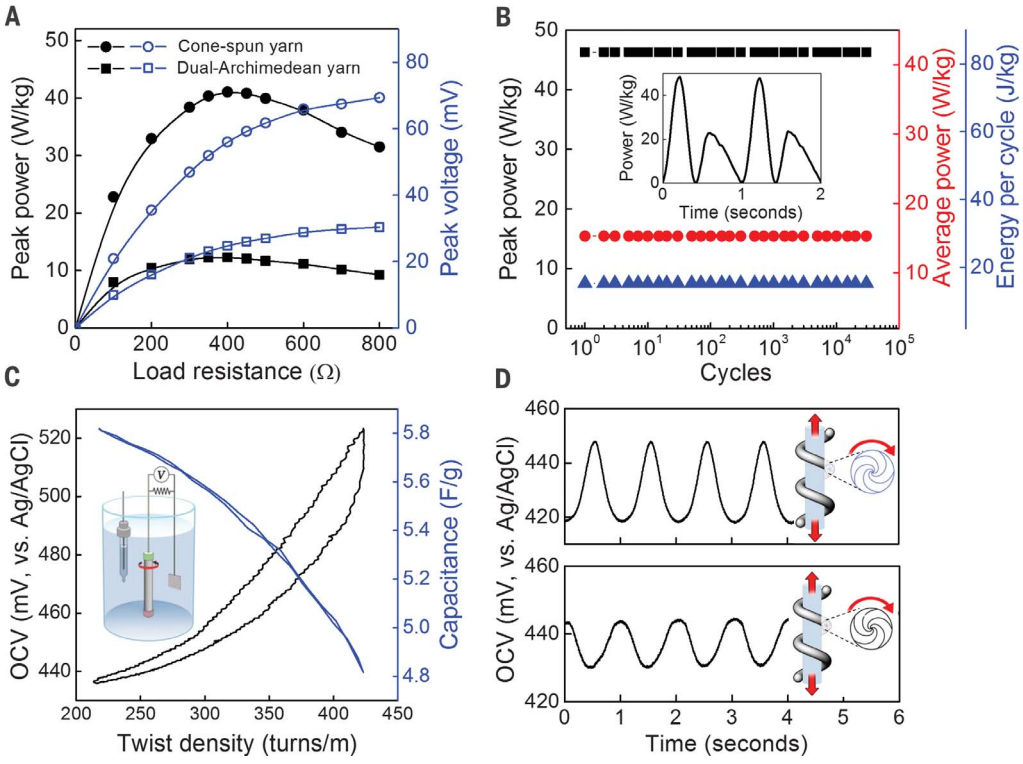

Fig. 2. Torsional and tensile performance of twistron harvesters. (**A**) Peak power (solid black symbols) and peak voltage (open blue symbols) versus load resistance for a 1-Hz stretch to 30% strain for the coiled harvester of Fig. 1C and for an otherwise identical dual-Archimedean–spun harvester. (**B**) Peak power, average power, and electrical energy per cycle during 30,000 stretch-and-release cycles to 30% strain at 1 Hz for the above twistron yarn in 0°C 0.6 M NaCl. (Inset) Output power versus time during typical cycles. (**C**) Dependence of capacitance and voltage on isometric twist and untwist for a noncoiled, 47-mm-long, 360-μm-diameter yarn in 0.1 M HCl. (Inset) Experimental apparatus. (**D**) OCV versus time during 60% stretch in 0.1 M HCl for homochiral (top) and heterochiral (bottom) yarns produced by mandrel coiling on a 300%-elongated, 0.5-mm-diameter rubber core, showing opposite stretch-induced voltage. (Insets) Opposite changes in yarn twist during stretch of homochiral and heterochiral coils.

energy. As shown in Fig. 2C and figs. S20 to S22 for isometric (constant-length) and isobaric (constant-force) twist insertion, respectively, twist insertion reversibly decreases the electrochemical capacitance and increases the OCV. The change in OCV is larger for isometric twist insertion (86.8 mV) than for isobaric twist insertion (43.6 mV), likely reflecting yarn densification and associated capacitance decrease during isobaric loading.

Inserting twist into a yarn until complete coiling occurs produces a "homochiral" yarn, because the twist to produce the noncoiled yarn and the subsequent yarn coiling are in identical directions. On the other hand, wrapping a twisted yarn around a mandrel can result in either homochiral or heterochiral coiled yarns, depending upon whether twist and coiling are in the same or opposite directions (*23*, *24*). When a homochiral coiled yarn is stretched, yarn coiling (called writhe) is partially converted to increased yarn twist, which increases yarn density (fig. S36), decreases yarn capacitance, and thereby increases the OCV. Opposite changes occur when stretching a heterochiral yarn. Although mechanical jigs can convert motion into an out-of-phase tensile deformation of two otherwise identical yarn electrodes, thereby doubling harvester voltage (figs. S26 to S28), we can avoid this mechanical complexity by using heterochiral and homochiral yarns as opposite twistron harvester electrodes. F3

Yarn coiling and twist can irreversibly cancel when stretching an unsupported heterochiral yarn. Consequently, dual–harvesting-electrode twistron harvesters utilized harvester yarns wrapped around a rubber fiber core, which acts as a return spring to prevent this irreversibility (*22*). Figure 2D shows the oppositely directed potential changes when stretching homochiral and heterochiral yarns, which further demonstrates that twist change is responsible for tensile energy harvesting by coiled yarns.

Harvesting without the need for an external bias voltage

Because a chemical potential difference exists between the harvester electrode and the surrounding electrolyte, immersing an electrode into an electrolyte generates an equilibrium charge on the electrode, which can be used for energy harvesting. The potential of zero charge (PZC) is needed for evaluating the equilibrium charge state of a twistron harvester. Because PZC measurements have been difficult and often inaccurate (*25*–*27*), we developed a method for measuring PZC, piezoelectrochemical spectroscopy (PECS). This method utilizes the charge-state–dependent response of a CNT electrode to mechanical deformation.

PECS involves characterizing an electrode by cyclic voltammetry (CV) while simultaneously stretching the electrode sinusoidally. Comparing CV scans with and without deformation, the dependence of the magnitude and phase of the stretch-induced ac current are determined versus applied potential (Fig. 3, A and B). From this plot, the PZC corresponds to the potential at which the ac current is minimized and the current's phase inverts by 180° (Fig. 3B). PECS showed that the PZC changes by less than ±7 mV from 3° to 60°C, which is important for harvesting energy from the ocean (Fig. 4C), and that the PZC changes by less than ±5 mV when a coiled twistron harvester is stretched by 20%. This result indicates that the charge injected by the electrolyte is largely independent of strain (Fig. 3D).

For twistron yarns, the intrinsic bias voltage (the difference between the PZC and the OCV at 0% strain) decreases with increasing pH (Fig. 3C). Hence, a low-pH electrolyte is hole-injecting, and a high-pH electrolyte is electron-injecting. Although the bias voltage depends on the specific electrolyte, even at the same pH, a linear dependence of bias voltage on pH was obtained (–47 mV per pH unit for aqueous HCl) (fig. S15, inset), consistent with the –59 mV per pH unit predicted by the Nernst equation (*28*). The direction of OCV change with applied tensile strain depends on whether the electrolyte provides a positive or negative bias potential (Fig. 3C). The OCV and peak power were maximized for 0.1 M HCl and 0.6 M NaCl concentrations (figs. S8 and S9).

Of the electrolytes investigated, 0.1 M HCl provides the highest chemically generated intrinsic bias voltage, ~0.4 V, and the greatest increase in yarn potential with stretch (150 mV for 30% strain) (Fig. 3C). This peak potential (550 mV) is close to that which causes hydrolysis of aqueous electrolytes, leaving little opportunity to increase power by providing an external bias voltage. Applying a 300-mV bias voltage during tensile energy harvesting in 0.1 M HCl (using 0.2-Hz square wave deformation to 20%), the net energy harvested per cycle increased from 17.9 to 27.1 $J \cdot kg^{-1}$ per cycle (fig. S14). Higher bias potentials decreased

the net harvested energy as electrolytic losses began to predominate.

The influence of yarn structure on electrochemical capacitance

Transmission electron microscopy (TEM) and scanning transmission electron microscopy (STEM) were used to assess the size, shape, and accessible surface area of individual CNTs and the bundles they form (*22*). Capacitances were calculated using the measured (*29*, *30*) areal capacitance of the basal plane of graphite (~4 μF/cm^2), which is close to that measured (*31*) for single-walled CNTs (~5 μF/cm^2) (*22*). Although Chmiola *et al.* have demonstrated that pore sizes with a radius smaller than the solvated ion can have an enhanced areal capacitance (*32*), the present calculations approximate the areal capacitance to be independent of pore size.

Even though TEM and STEM images show that most nanotubes are bundled (Fig. 5, A and B), the measured capacitances in Fig. 2C and fig. S20 (5.8 F/g and 8.3 F/g for the partially twisted and nontwisted torsional harvesters, respectively) are close to those theoretically estimated for fully nonbundled MWNTs (9.7 F/g) (fig. S32) (*22*). This is explained by our observation that bundled MWNTs are far from cylindrical (Fig. 5, A and B, and fig. S35) (*22*) and that bundles have sufficiently large pores to accommodate electrolyte ions such as hydrated Na^+ and Cl^- (figs. S33 and S34). This electrolyte penetration occurs despite the fact that the investigated MWNTs are partially collapsed to gain internanotube van der Waals energy (Fig. 5A) instead of being noncollapsed or fully collapsed (*33*, *34*) to gain the van der Waals energy of the innermost nanotube wall.

To investigate how increasing twist causes reversible changes in yarn capacitance, we performed empirical–force-field molecular dynamics simulations on a typical observed bundled structure to predict the effect of twist-induced pressure on intrabundle void space (*22*). Using biaxial pressures up to 50 MPa, which agree with the measured torques required for twisting, a reversible 26% change in intrabundle capacitance (from 2.6 to 1.9 F/g) was calculated (figs. S37 to S39) (*22*), which is similar to the percent capacitance change seen experimentally during energy harvesting.

Twistron applications and comparisons to other harvesters

Transitioning from electrolyte-bath–operated harvesters to harvesters that operate in air is important. We fabricated one such device by first overcoating a coiled CNT yarn with a gel electrolyte [including 10 weight % (wt %) polyvinyl alcohol (PVA) in 0.1 M HCl], which did not degrade output power (fig. S29). Then a noncoiled, twisted, CNT yarn counter electrode, coated with an ionically conducting hydrogel to prevent shorting, was helically wrapped around the energy-harvesting electrode (i.e., fig. S30). Finally, this combined two-electrode assembly was overcoated with the PVA/HCl gel electrolyte to yield the peak voltage and peak harvested power shown in Fig. 4A.

To produce liquid-electrolyte–free harvesters that generate energy from both electrodes, we used the homochiral and heterochiral yarns of Fig. 2D. Three pairs of these homochiral and heterochiral yarns were separately sewn into a knitted cotton glove, with a 1.5-mm interelectrode separation that matched the periodicity of the knit, and each electrode pair was then separately overcoated with a PVA/LiCl gel electrolyte. Figure 4B shows their performance when connected in parallel and in series when the textile is stretched by 50%. We demonstrated application of the twistron harvester of Fig. 4B as a self-powered solid-state strain sensor that is sewn into a shirt and used for monitoring breathing (fig. S31 and movie S1).

Figure 4C shows the results of an initial effort to harvest the energy of near-shore ocean waves. Both an energy harvesting coiled twistron yarn and a Pt mesh/CNT counter electrode were directly immersed in the Gyeonpo Sea off South Korea, where the ocean temperature was 13°C, the NaCl content was 0.31 M, and the wave frequency during the study ranged from 0.9 to 1.2 Hz. The yarn was attached between a balloon and a sinker on the seabed. Using a 10-cm-long twistron harvester electrode weighing 1.08 mg, whose deformation was mechanically limited to 25%, a peak-to-peak open-circuit voltage of 46 mV and an average output power of 1.79 μW were measured during ocean-wave harvesting. The average output power through a 25-ohm load resistor (normalized to the harvester electrode weight) was 1.66 W/kg.

Our harvester yarns can provide arbitrarily high voltages if multiple harvesters are combined in series, as in Fig. 4B, or commercially available circuits are used to increase harvester voltage. For instance, the ~80-mV output voltage of a single coiled harvester electrode (weighing 19.2 mg)

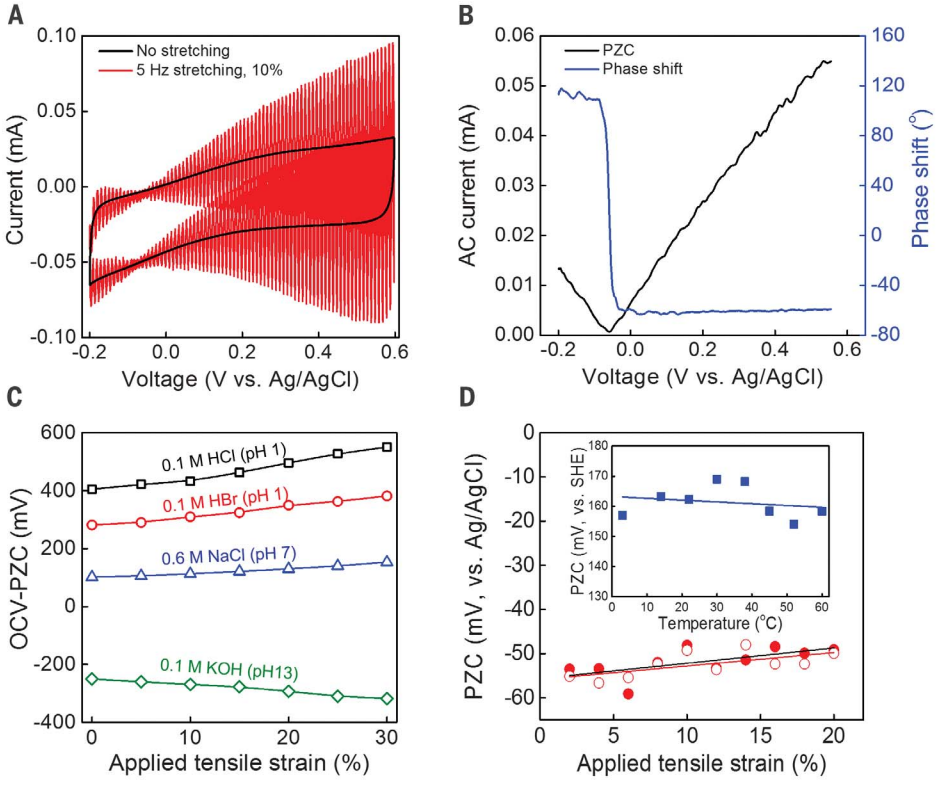

Fig. 3. Piezoelectrochemical spectroscopy and its application for twistron harvesters. (**A**) Cyclic voltammograms (50-mV/s scan rate) of a coiled twistron electrode in 0.1 M HCl during a 5-Hz sinusoidal stretch to 10% (red) and without deformation (black). (**B**) Magnitude and phase of current fluctuations relative to the applied mechanical stretch. The potential of both the minimum current amplitude and the 180° phase shift correspond to the potential of zero charge (PZC) (−58 mV versus Ag/AgCl). (**C**) OCV (versus PZC) in different electrolytes for 1-Hz strain, indicating the combined effects of chemically induced charge injection and stretch-induced capacitance change. (**D**) Negligible dependence of PZC on applied strain for increasing (solid) and decreasing (open) strain and temperature (inset). SHE, standard hydrogen electrode.

charged a 5-μF capacitor to 2.8 V using a voltage step-up converter (fig. S40 and Fig. 4D). Movie S2 shows this harvester powering a green light–emitting diode, which lights up to indicate each time the harvester yarn is stretched.

We previously used polymer artificial muscles to convert temperature fluctuations into mechanical energy, which was harvested as electrical energy using an electromagnetic generator (*35*). Unfortunately, the large weight and volume of the electromagnetic generator dwarfs the polymer muscle, and these electromagnetic generators suffer from low gravimetric and volumetric power output when downsized (*36*). Twistron harvesters can be used to solve this problem because they can be smaller in diameter than a human hair and have much smaller weight and volume than the polymer muscle used to convert thermal energy to mechanical energy. A thermally annealed coiled–nylon-fiber artificial muscle was attached to a coiled twistron harvester with the same twist direction. Heating the nylon muscle both up-twists and stretches the twistron harvester, additively contributing to energy generation. Upon heating from room temperature to 170°C in 1 s, followed by air cooling for 2 s, actuation of a 10-cm-long coiled-nylon muscle drove the 2-cm-long twistron yarn to deliver a peak electrical power of 40.7 W/kg, relative to twistron weight (Fig. 4E). Considering the entire system weight, including both the weight of the actuating nylon yarn and the 28-fold lower weight of the twistron energy harvester, this corresponds to 1.41 W/kg of peak electrical power and 0.86 W/kg of average power during heating and a full-cycle average electrical power of 0.29 W/kg, compared with 0.015 W/kg for a polymer muscle connected to an electromagnetic generator (*36*). Small temperature fluctuations can be harvested by increasing the polymer muscle length, such as by using pulleys to minimize total package size or by using large–spring-index polymer muscle coils to maximize stroke (*37*).

A twistron harvester's output power is limited by its electrical impedance. Although the full equivalent harvester circuit is complex, a simple *R-C* model can qualitatively describe the main observed features. In this approximation, the harvester impedance is $Z_{harvester} = R_{internal} + 1/(j\omega C)$, where j is $\sqrt{-1}$ and ω is the angular frequency. At low stretch frequencies, this impedance is dominated by the double-layer capacitance ($Z_c = 1/j\omega C$), leading to the observed rise in power with increasing frequency (Fig. 1E and fig. S10). At higher frequencies, where capacitor impedance is minimal, internal resistance ($R_{internal}$) dominates, and power output versus frequency reaches a plateau.

A major performance increase resulted from our discovery that yarn resistance was contributing to twistron impedance (fig. S12). Peak power for 50% stretch at 12 Hz was increased from 179 W/kg (Fig. 1E) to 250 W/kg (Fig. 4D and fig. S16) by coiling a 23-μm-diameter Pt wire within the coiled twistron yarn. Though it did not substantially affect the stress-strain curve of the elastically stretched harvester (fig. S17), the presence of the conducting wire also increased the average output electrical power for 12-Hz sinusoidal deformation from 39 to 56 W/kg. On the basis of this average power output, just 31 mg of CNT yarn harvester could provide the average power needed to transmit a 2-kB packet of data over a 100-m radius every 10 s (*38*) for the Internet of Things.

Figure 5, C and D, and table S2 compare the gravimetric power densities of our tensile twistron harvesters to alternative microscale or macroscale technologies, some of which have had decades

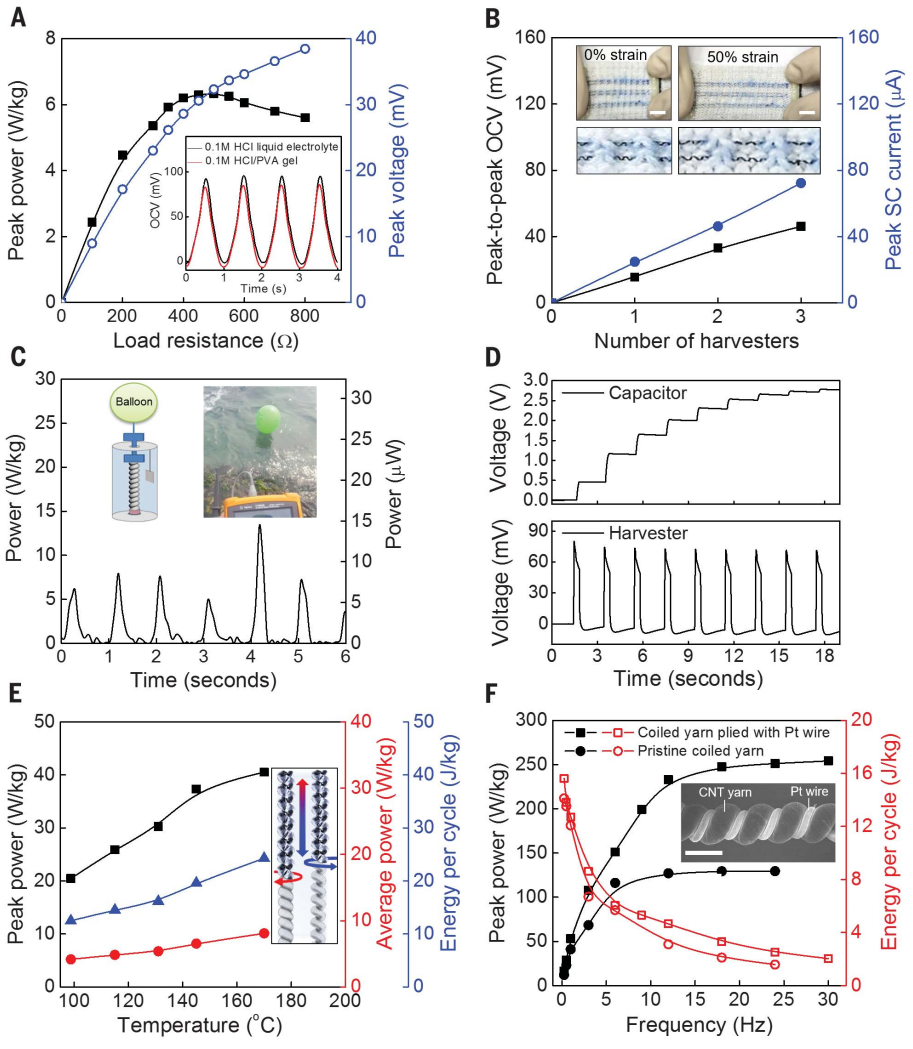

Fig. 4. Alternative harvester geometries. (**A**) Peak power per device weight and peak voltage versus load resistance for 1-Hz, 30% stretch of a harvesting coiled CNT yarn working electrode that is coated with 0.1 M HCl–containing polyvinyl alcohol (PVA) gel and wrapped with a nonharvesting, PVA/HCl-coated, noncoiled CNT yarn counter electrode. (Inset) OCV versus time, before and after PVA coating. (**B**) Peak-to-peak OCV and peak SCC at 1 Hz and 50% strain for series (black squares) and parallel (blue circles) connected harvesters using homochiral and heterochiral yarn pairs. The yarns were coated with a 10–wt % PVA/4.5 M LiCl gel electrolyte after being sewn into a textile. (Inset) Photographs of the textile at 0 and 50% strain (scale bars, 1 cm). (**C**) Gravimetric and absolute power output of a 1.08-mg twistron ocean-wave harvester for wave frequencies of 0.9 to 1.2 Hz. The average power was 1.79 μW. (Insets) The harvester configuration, which was tethered to the ocean floor and mechanically limited to <25% stretch, and a photograph taken during harvesting. (**D**) Data from charging a 5-μF capacitor to 2.8 V using a CNT yarn harvester (weighing 19.2 mg) and a boost converter circuit. The capacitor voltage and the harvester voltage are shown during a 0.5-Hz square wave stretch to 14% strain at 20% duty. The boost converter output was rectified through a Schottky diode before charging the capacitor. (**E**) Peak power (black squares), average power (red circles), and energy per cycle (blue triangles) generated by a coiled twistron harvester when stretched and twisted by an in-series, coiled, 127-μm-fiber-diameter nylon artificial muscle (above the electrolyte) that converts thermal energy into mechanical energy. (Inset) Illustration of twistron up-twist and stretch during muscle heating and the reverse processes during muscle cooling. (**F**) Frequency dependence of peak power (black symbols) and energy per cycle (red symbols) before and after incorporating a Pt wire current collector into a coiled twistron yarn. (Inset) Scanning electron microscopy image of this harvester (scale bar, 100 μm).

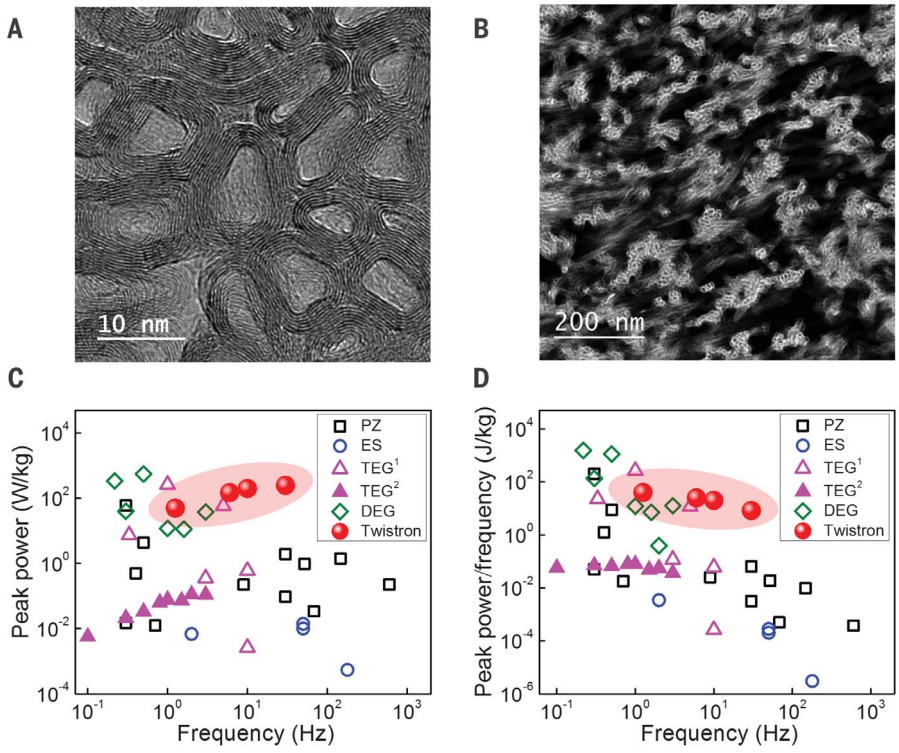

Fig. 5. Structural origin of twistron performance and comparisons with previously known material-based harvesters. (**A**) TEM image showing multiwalled nanotube (MWNT) collapse to increase internanotube van der Waals energy in a MWNT bundle. (**B**) STEM image showing the high surface area of MWNT bundles. (**C** and **D**) Peak power (C) and frequency-normalized peak power (D) versus the frequency at which this peak power was obtained for present and prior-art technologies for piezoelectric (PZ), electrostatic (ES), triboelectric (TEG^1), and dielectric elastomer (DEG) generators (*22*). The solid triangles represent the low-frequency triboelectric data (TEG^2) of Zi *et al*. (*36*).

or centuries to mature. For stretch frequencies between a few hertz and 600 Hz, we could find no other material-based harvesting technology that provides a higher reported peak power or frequency-normalized peak power than our twistron harvesters. At very high frequencies, Zhu *et al.* (*39*) have reported that triboelectric harvesters can generate noteworthy average power outputs (1.27 kW/kg at 1 kHz and 5 kW/kg at 5 kHz, which correspond to frequency-normalized average power values of 1.27 and 1.00 J/kg, respectively). Extrapolation to lower frequencies, using the reported approximately linear dependence of average power on frequency for these triboelectric harvesters, suggests that they should provide a higher average power density than twistron harvesters for frequencies >100 Hz (*37*).

The high gravimetric output power of twistron harvesters reflects the high gravimetric mechanical energy that can be input during stretch (1.67 kJ/kg for 20% strain), rather than a high mechanical-to-electrical energy conversion efficiency. In fact, simultaneous measurement of tensile mechanical energy input and electric energy output during cycling of a coiled twistron yarn at 1 Hz to 20% strain in 0.1 M HCl resulted in an energy conversion efficiency of only 1.05% for this first generation of twistron harvesters (fig. S19).

Future application of the twistron harvesters might result from their high gravimetric power densities, the giant stroke range over which mechanical energy can be harvested, the broad frequency range over which these harvesters provide high power, their operation in seawater and other electrolytes without the need for an external bias potential, and their scalability from micrometer-scale–diameter harvesters in textiles to parallel devices that harvest ocean energy. The low mechanical-to-electrical conversion efficiency of the twistron harvesters is a present problem for applications in which high gravimetric output power is less important than energy conversion efficiency.

REFERENCES AND NOTES

1. S. Beeby, T. O'Donnell, "Electromagnetic energy harvesting" in *Energy Harvesting Technologies*, S. Priya, D. Inman, Eds. (Springer, 2009).
2. L. Persano *et al.*, *Nat. Commun.* **4**, 1633 (2013).
3. Z. L. Wang, J. Song, *Science* **312**, 242–246 (2006).
4. S. Niu, X. Wang, F. Yi, Y. S. Zhou, Z. L. Wang, *Nat. Commun.* **6**, 8975 (2015).
5. W. Tang *et al.*, *ACS Nano* **9**, 7867–7873 (2015).
6. J. Yin *et al.*, *Nat. Nanotechnol.* **9**, 378–383 (2014).
7. S. Ghosh, A. K. Sood, N. Kumar, *Science* **299**, 1042–1044 (2003).
8. J. W. Liu, L. M. Dai, J. W. Baur, *J. Appl. Phys.* **101**, 064312 (2007).
9. T. Park, C. Park, B. Kim, H. Shin, E. Kim, *Energy Environ. Sci.* **6**, 788–792 (2013).
10. S. Kim *et al.*, *Nat. Commun.* **7**, 10146 (2016).
11. M. Aureli, C. Prince, M. Porfiri, S. D. Peterson, *Smart Mater. Struct.* **19**, 015003 (2010).
12. T. Krupenkin, J. A. Taylor, *Nat. Commun.* **2**, 448 (2011).
13. J. K. Moon, J. Jeong, D. Lee, H. K. Pak, *Nat. Commun.* **4**, 1487 (2013).
14. R. Pelrine *et al.*, *Proc. SPIE* **4329**, 148 (2001).
15. S. Chiba, M. Waki, R. Kornbluh, R. Pelrine, *Proc. SPIE* **2008**, 692715 (2008).
16. T. Mirfakhrai *et al.*, *Adv. Sci. Tech.* **61**, 65–74 (2008).
17. M. Zhang, K. R. Atkinson, R. H. Baughman, *Science* **306**, 1358–1361 (2004).
18. M. Zhang *et al.*, *Science* **309**, 1215–1219 (2005).
19. X. Lepró *et al.*, *Adv. Funct. Mater.* **22**, 1069–1075 (2012).
20. S. Priya *et al.*, *Energy Harvesting Syst.* **4**, 3–39 (2017).
21. M. D. Lima *et al.*, *Science* **331**, 51–55 (2011).
22. See supplementary materials.
23. M. D. Lima *et al.*, *Science* **338**, 928–932 (2012).
24. C. S. Haines *et al.*, *Science* **343**, 868–872 (2014).
25. M. Kosmulski, *J. Colloid Interface Sci.* **337**, 439–448 (2009).
26. L. H. Shao *et al.*, *Phys. Chem. Chem. Phys.* **12**, 7580–7587 (2010).
27. E. McCafferty, *Electrochim. Acta* **55**, 1630–1637 (2010).
28. Y. Tanaka *et al.*, *Angew. Chem. Int. Ed.* **48**, 7655–7659 (2009).
29. J. P. Randin, E. Yeager, *J. Electrochem. Soc.* **118**, 711–714 (1971).
30. J. P. Randin, E. Yeager, *J. Electroanal. Chem. Interfacial Electrochem.* **36**, 257–276 (1972).
31. J. N. Barisci, G. G. Wallace, D. Chattopadhyay, F. Papadimitrakopoulos, R. H. Baughman, *J. Electrochem. Soc.* **150**, E409–E415 (2003).
32. J. Chmiola *et al.*, *Science* **313**, 1760–1763 (2006).
33. M. Motta, A. Moisala, I. A. Kinloch, A. H. Windle, *Adv. Mater.* **19**, 3721–3726 (2007).
34. M. F. Yu, M. J. Dyer, R. S. Ruoff, *J. Appl. Phys.* **89**, 4554–4557 (2001).
35. S. H. Kim *et al.*, *Energy Environ. Sci.* **8**, 3336–3344 (2015).
36. Y. Zi *et al.*, *ACS Nano* **10**, 4797–4805 (2016).
37. C. S. Haines *et al.*, *Proc. Natl. Acad. Sci. U.S.A.* **113**, 11709–11716 (2016).
38. W. R. Heinzelman, A. Chandrakasan, H. Balakrishnan, "Energy-efficient communication protocol for wireless microsensor networks," in *Proceedings of the 33rd Hawaii International Conference on System Sciences* (IEEE, 2000), p. 8020.
39. G. Zhu *et al.*, *Adv. Mater.* **26**, 3788–3796 (2014).

ACKNOWLEDGMENTS

We thank B. Buckenham, A. M. Baughman, and N. K. Mayo for preparing samples and performing measurements. This work was supported in Korea by the Creative Research Initiative Center for Self-Powered Actuation of the National Research Foundation of Korea and the Ministry of Science, ICT & Future Planning, the Korea–U.S. Air Force Cooperation Program (grant 2013K1A3A1A32035592), and a KETEP grant (20168510011350) grant of the Ministry of Knowledge Economy. In the United States, this work was supported by Air Force Office of Scientific Research grants (FA9550-15-1-0089 and FA9550-12-1-0035), an Air Force grant (AOARD-FA2386-13-4119), a NASA project (NNX15CS05C), a Robert A. Welch Foundation grant (AT-0029), and an Office of Naval Research grant (N00014-14-1-0158). S.H.K., C.S.H., N.L., S.F., J.D., K.J.K., T.J.M., C.C., S.J.K., and R.H.B. are the inventors of provisional U.S. patent application no. 62/526,188, submitted jointly by the Board of Regents, the University of Texas System (for the University of Texas at Dallas), and the Industry-University Cooperation Foundation of Hanyang University, that covers the design, fabrication, performance, and applications of twistron mechanical energy harvesters.

SUPPLEMENTARY MATERIALS

www.sciencemag.org/content/357/6353/773/suppl/DC1
Materials and Methods
Supplementary Text
Figs. S1 to S40
Tables S1 and S2
References (*40*–*79*)
Movies S1 and S2

3 February 2017; accepted 21 July 2017
10.1126/science.aam8771

Science

Harvesting electrical energy from carbon nanotube yarn twist

Shi Hyeong Kim, Carter S. Haines, Na Li, Keon Jung Kim, Tae Jin Mun, Changsoon Choi, Jiangtao Di, Young Jun Oh, Juan Pablo Oviedo, Julia Bykova, Shaoli Fang, Nan Jiang, Zunfeng Liu, Run Wang, Prashant Kumar, Rui Qiao, Shashank Priya, Kyeongjae Cho, Moon Kim, Matthew Steven Lucas, Lawrence F. Drummy, Benji Maruyama, Dong Youn Lee, Xavier Lepró, Enlai Gao, Dawood Albarq, Raquel Ovalle-Robles, Seon Jeong Kim and Ray H. Baughman

Science **357** (6353), 773-778.
DOI: 10.1126/science.aam8771

Making the most of twists and turns

The rise of small-scale, portable electronics and wearable devices has boosted the desire for ways to harvest energy from mechanical motion. Such approaches could be used to provide battery-free power with a small footprint. Kim *et al.* present an energy harvester made from carbon nanotube yarn that converts mechanical energy into electrical energy from both torsional and tensile motion. Their findings reveal how the extent of yarn twisting and the combination of homochiral and heterochiral coiled yarns can maximize energy generation.

Science, this issue p. 773